

A Theoretical Model of Glucose Transport Suggests Symmetric GLUT1 Characteristics at Placental Membranes

Efrath Barta · Ariele Drugan

Received: 19 March 2014 / Accepted: 13 May 2014 / Published online: 4 June 2014
© Springer Science+Business Media New York 2014

Abstract The process of glucose transport via the placenta is not fully deciphered. Here, we apply a theoretical model to compute glucose fluxes via the terminal villi of the human placenta for various sets of parameter values and conclude on characteristics of transport across the two bordering membranes. Based on available measured data, the spatial geometry of the terminal villi is being simulated. Within this region, glucose concentrations and fluxes are computed by a numerical scheme that solves the diffusion equation with boundary conditions that account for transporter mediated diffusion at the membranes. Feasible parameter values (ones that induce physiological glucose fluxes) are determined for four optional symmetry characteristics of the membranes. Confronting computed results with clinical knowledge reveals the most plausible scenario-symmetric activity of the transporter at the microvillous membrane. Thus, sensitivity analysis of the computed results enables deduction about micro-scale mechanisms at the bordering membranes based on macro-scale knowledge.

Keywords Facilitated transport · Glucose uptake · GLUT1 activity · Mathematical modeling · Terminal villi membranes

Introduction

There are ample evidences as for the importance and complexity of the glucose transport from maternal blood via the human placenta to fetal blood. Unfortunately, our understanding of this transport process that involves many factors is far from being satisfactory (Day et al. 2013). The huge differences between epitheliochorial placenta (as in sheep) and hemochorial placenta (as in human) obstruct extrapolation from one species to another (Sibley and Boyd 1979) and human *in vivo* measurements are impossible to carry on. The different, sometimes contradictory, evidences from *in vitro* studies call for a rigorous theoretical study that might elucidate the *in vivo* situation.

Due to the highly irregular shape of the placenta (the villi are constructed as hierarchical trees with splitting branches where each villus is penetrated by fetal capillaries), it is impossible to have an analytic description of the placental morphometry. Moreover, the high variability of placental morphometry across normal gravid women turns pointless any effort to determine a “universal” shape. This is why existing transport models are 1-D ones and refer to the placenta as a simple barrier, ignoring its metabolic consumption and/or the activity of transporters (Simmons et al. 1979; Hay et al. 1990; Barta and Drugan 2010). Here, we aim to do better by analytically defining an isolated terminal villus and then simulating the glucose transport across it. As toward term the terminal villi that are bathed in maternal blood are the most important site for diffusional exchange (Benirschke et al. 2012), this simulation might approximate the placental glucose transport process in spite of ignoring the effects of neighboring villi and other components of the placental barrier.

The permeation of glucose, either at the microvillous membrane (MVM) where the glucose enters the villous

E. Barta (✉)
Bar-Code Computers Ltd, PO Box 2013, 3912001 Tirat-Carmel,
Israel
e-mail: efrathb@gmail.com

A. Drugan
Department of Obstetrics and Gynecology, Rambam Health Care Campus, The Rappaport Faculty of Medicine, Technion Institute of Technology, PO Box 9602, 3109601 Haifa, Israel

tree or at the basal membrane (BM) where it enters the fetal blood, has two parallel routes: a simple diffusion and a diffusion facilitated by GLUT1, a specific glucose transporter that associates the glucose and is abundant at the two membranes of the terminal villi (Jansson et al. 1999; Baumann et al. 2002; Desoye et al. 2011). The second mechanism is dominant, because the membranes, due to their high lipids content, have a low permeability with respect to the free molecules of glucose. Qualitatively, according to the single site exposure (simple carrier) model of facilitated diffusion, the translocation starts with a reaction of the glucose with an exofacial binding site (actually there are indications for the existence of 2–3 binding sites (Gould and seatter 1997)) on the outer face of the membrane. Then, the complex molecule is transported via a conformational change within the protein so that it faces the inner side of the membrane where the glucose dissociates and is available to the cytoplasm. The same occurs on the opposite direction, i.e., the glucose binds to the endofacial site, and via a re-orientation process is transferred to the outer face of the membrane. The different conditions that prevail at the two faces of the membranes and the asymmetry between various rate constants and transporter concentrations result in the net flux of the glucose. Most of the involved parameters have never been measured; therefore, we tried to estimate their values based on data taken from erythrocytes membranes.

We run the simulation for a wide range of parameter values, all within the feasible range, i.e., they all induce physiological fluxes of glucose. Confronting the predictions of this model with clinical knowledge regarding the sensitivity of the glucose fluxes with respect to GLUT1 and glucose concentrations helps to choose the most probable transport characteristics at the membranes. Specifically, we prove that realistic glucose transport involves symmetric GLUT1-related features of the MVM. Thus, this simulation that entails knowledge regarding the glucose transport on the macro-scale (the *in vivo* whole placenta) enables deduction regarding the micro-scale mechanisms (the characteristics of the GLUT1 activity at specific membranes).

The Mathematical Model

Simulating the Region of Solution

Terminal villi come with a huge variability of shapes but essentially they look like elongated grapes (i.e., truncated spheroids) whose outer surface is the MVM, a membrane with dense, slender microvilli on its face. Within the terminal villi lie the fetal capillaries that are engulfed by the BM. The variability of those capillaries (their number, their

radii and branching patterns) is so high that one would better relate to their “envelope,” the basal lamina that toward term sticks to the BM of the trophoblast, than to them specifically (Jirkovska et al. 1998, 2008, 2012). That is why we define, based on global measurements, a spheroid that tightly “packs” the capillaries instead of trying to simulate the capillaries themselves.

Notable are the high discrepancies in the measurements of both area and volumetric capillaries to villi ratios, as appear in Table 1. Those might be attributed to the varied osmolarities of the fixative in which the specimens of the placenta were immersed as well as to different definitions of capillaries volume (some refer to the lumen and some to the whole capillary), different definitions of the peripheral villi (including or not the intermediate villi) and to the time of cord clamping.

Using the transformation from a cartesian (x, y, z) system of coordinates to a spheroidal (ξ, η, φ) one:

$$\begin{aligned} x &= a \operatorname{Sinh}[\xi] \times \operatorname{Sin}[\eta] \times \operatorname{Cos}[\varphi] \\ y &= a \operatorname{Sinh}[\xi] \times \operatorname{Sin}[\eta] \times \operatorname{Sin}[\varphi] \\ z &= a \operatorname{Cosh}[\xi] \times \operatorname{Cos}[\eta] \end{aligned} \quad (1)$$

and the measured relevant characteristics of the placenta, summarized in Table 1, we model a “representative” isolated terminal villus as a truncated spheroid, see Fig. 1.

Assuming that the neck region of the villus (where it attaches to the mature intermediate villus) has a radius of about 0.7 of its equatorial radius, one may easily define the characteristic parameters of the two confocal spheroids, the outer one that stands for the MVM and the inner one that represents the BM, as is summarized in Table 2. It is essential that those two spheroids will be confocal (i.e., share the same a value in Eq. 1) in order to enable utilization of a unique spheroidal coordinate system throughout the entire region of solution.

The parameter values in Table 2 induce a villus with a volume of 1.38×10^{-7} ml and a surface area of 1.43×10^{-4} cm². Thus, we conclude that the placenta contains about 8.5×10^8 terminal villi.

The thickness of the trophoblastic barrier in the simulated villus varies from 1.54 μ m at the apex to 5.66 μ m at the equatorial plane, in accord with measured averaged thickness of 4 μ m (Sibley and Boyd 1979; Jackson et al. 1992; Jauniaux and Burton 2006; Day et al. 2013).

Microvilli are spread all over the MVM, serving as a booster for the uptake process by considerably increasing the area where the transport occurs (Demir 1979; Truman et al. 1981; Ibrahim et al. 1982; Karimu and Burton 1995). Their distribution on the membrane is a controversial subject—some claim that the MVM is covered almost homogenously by the microvilli (Karimu and Burton 1995), while others detected densely covered regions and

Table 1 Morphometric data used for the simulation of a terminal villus in normal full-term human placenta

Parameter	Chosen value	Measured values
Radius of a terminal villus	22 μm	15–35 μm^{a}
Length of a terminal villus	121 μm	4–7 times the radius ^b
Surface area of peripheral villi	12 m^2	9–16 m^2 ^c
Fetal capillaries to peripheral villi surface area ratio	0.72	0.68–1.1 ^d
Trophoblast to terminal villi volume ratio	0.45	0.35–0.75 ^e
Radius of a microvillus	0.055 μm	^f
Length of a microvillus	0.6 μm	^f
Spacing between adjacent microvilli	0.215 μm	^g

^a Sen et al. 1979; Honda et al. 1992; Jackson et al. 1992; Mayhew et al. 1994

^b Jirkovska et al. 1998

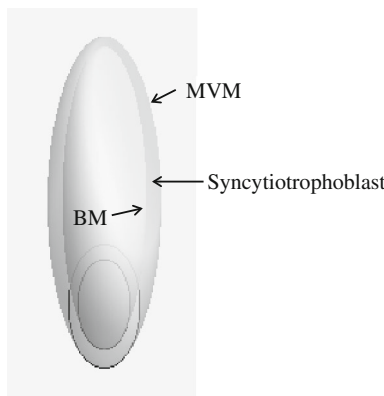
^c Aherne and Dunnill 1966; Laga et al. 1973; Teasdale and Jean-Jacques 1985; Mayhew 2003; Jauniaux and Burton 2006; Higgins et al. 2011

^d Aherne and Dunnill 1966; Sibley and Boyd 1979; Jackson et al. 1992; Mayhew et al. 1994

^e Sen et al. 1979; Mayhew 2003; Jauniaux and Burton 2006

^f Teasdale and Jean-Jacques 1985

^g Demir 1979

**Fig. 1** A simulated terminal villus. The shaded thin shell represents the syncytiotrophoblast, the region where the differential equation is applied. The ring at the bottom is the site of attachment to the intermediate villus

regions that are devoid of microvilli (Ibrahim et al. 1982). In addition, their shape and size were shown to vary. Therefore, the least speculative way to account for the microvilli presence is to estimate their effect on the total surface area of the membrane and multiply the permeability constant at the MVM by this enlargement factor.

We estimate this enlargement factor as follows: Imagine a squared piece of membrane, its side measures l_e , with a cylindrical-shaped microvillus located at its center. The

Table 2 Geometrical parameter values for a model of a terminal villus in human-term placenta

Parameter	value	Comments
a	68 μm	The same a value is shared by the MVM and the BM
ξ_m	0.32	ξ_m and η_m define the MVM
η_m	2.342 rad	
ξ_b	0.24	ξ_b and η_b define the BM
η_b	2.349 rad	
E	5.5	Enlargement factor due to the presence of the microvilli

surface area of this unit will be $\{1 + 2\pi \times 0.055 \times 0.6/l_e^2\}$ times the surface area of a similar squared piece with no attached microvillus. $l_e = 0.215 \mu\text{m}$ (see Table 1), and consequently, we deduce that the presence of the microvilli multiplies the overall MVM surface area by a factor E , $E = 5.5$.

Formulation of the Boundary Value Problem

Glucose diffuses via the cytoplasm of the syncytiotrophoblast, the space confined in each terminal villus between the MVM and the BM. Therefore, glucose concentration is given by a solution of the diffusion-consumption equation:

$$D \nabla^2 C_g = k_g C_g \quad (2)$$

where ∇^2 stands for the Laplacian operator, and D is the diffusion coefficient of the glucose that has a spatial concentration C_g within the cytoplasm. k_g is the glucose consumption rate constant. Transient fluctuations of concentrations might be accounted for by including temporal derivative in the above equation but, as was discussed in Barta and Drugan (2010), they have a minor clinical relevance and therefore are ignored here. Using the prolate spheroidal coordinates system (ξ, η, φ) defined in Eq. 1, Eq. 2 is written as

$$\frac{D}{a^2(\text{Sinh}^2[\xi] + \text{Sin}^2[\eta])} \left\{ \frac{1}{\text{Sinh}[\xi]} \frac{\partial}{\partial \xi} \left(\text{Sinh}[\xi] \frac{\partial C_g}{\partial \xi} \right) + \frac{1}{\text{Sin}[\eta]} \frac{\partial}{\partial \eta} \left(\text{Sin}[\eta] \frac{\partial C_g}{\partial \eta} \right) \right\} + \frac{D}{a^2 \text{Sinh}^2[\xi] \text{Sin}^2[\eta]} \frac{\partial^2 C_g}{\partial \varphi^2} = k_g C_g \quad (3)$$

Due to axial symmetry, the last term on the left-hand side of Eq. 3 is null, and the solution is valid for every circumferential (φ) position. The region of solution extends from $\xi = \xi_b$, $0 \leq \eta \leq \eta_b$ to $\xi = \xi_m$, $0 \leq \eta \leq \eta_m$.

The diffusion equation has to be supplemented with the following:

- I. A boundary condition at the base of the villus that represents a smooth, continuous move from the terminal villus to the mature intermediate villus. In other words, the diffusion equation is assumed to be satisfied in the attached intermediate villus as well.
- II. Boundary conditions at the two membranes: The flux is proportional to the component of the gradient of concentration that is normal to the surface which is in case of ellipsoidal surfaces—the partial derivative along the ξ direction. Thus, we satisfy for $\xi = \xi_m$, $0 \leq \eta \leq \eta_m$ (at the MVM):

$$\frac{D}{a\sqrt{\text{Sinh}^2[\xi] + \text{Sin}^2[\eta]}} \frac{\partial C_g}{\partial \xi} = E(k_{oMVM}(C_{ggl}^m - \text{prop}_{MVM}C_{ggl}^{pm}) + P_{0g}((C_g^m - C_{ggl}^m) - (C_g - C_{ggl}^{pm}))) \quad (4)$$

and at the BM where $\xi = \xi_b$, $0 \leq \eta \leq \eta_b$:

$$\frac{D}{a\sqrt{\text{Sinh}^2[\xi] + \text{Sin}^2[\eta]}} \frac{\partial C_g}{\partial \xi} = k_{oBM}(C_{ggl}^{pf} - \text{prop}_{BM}C_{ggl}^f) + P_{1g}((C_g - C_{ggl}^{pf}) - (C_g^f - C_{ggl}^f)) \quad (5)$$

where k_{oMVM} and k_{oBM} are translocation rate constants at the two membranes, prop_{MVM} and prop_{BM} are proportion constants that represent the asymmetry between the translocation rates along the in and out directions within the membranes, C_{ggl}^m and C_{ggl}^{pm} are concentrations of the glucose-GLUT1 complex at the maternal and placental faces of the MVM, respectively, and C_{ggl}^{pf} , C_{ggl}^f are the concentrations of the glucose-GLUT1 complex at the placental and fetal faces of the BM respectively. C_g^m and C_g^f are the glucose concentrations in the maternal and fetal blood, respectively. P_{0g} and P_{1g} are the permeability constants of the MVM and the BM with respect to the free glucose.

As the reactions that involve association or dissociation of GLUT1 and glucose are much faster than the re-orientation mechanism, one may assume them to be so fast that all constituents: transporter, glucose, and their complex are in an equilibrium at membranes faces, and concentration of the complex molecule is defined as a solution of a quadratic equation (Barta and Drugan 2010).

Note that in Eq. 4, the permeability constants are multiplied by the enlargement factor, E in order to account for the microvilli presence.

The Numerical Procedure

Unable to locate an off the shelf routine that solves the above boundary value problem, we defined a numerical

scheme as follows: Grid points are densely scattered in order to span the cross section of the syncytiotrophoblast of a terminal villus. At these points, the diffusion equation is written with derivatives being approximated by central, second-order differences. The resulting system of algebraic equations is solved by the `FindRoot` function of the `Mathematica` software library. It is verified that convergence occurs using 100 grid points along each (η and ξ) direction. The solution of the equations, a map of glucose concentration throughout the syncytiotrophoblast, serves to compute glucose fluxes at the membranes.

Parameter values

Our model incorporates many parameters—some of them were defined in previous works, but most of them should be assessed here:

* k_g , the consumption rate constant is computed based on measured total glucose consumption rate of $4\text{--}10 \mu\text{M} (\text{hr} \times \text{g})^{-1}$ near term (Villee 1953; Ogburn et al. 1988). A similar range of glucose utilization rates is deduced from the measurements of Hauguel et al. (1986). Assuming that glucose concentration within the villus is close to the maternal level (Barta and Drugan 2010) and that most of the placental consumption occurs within the trophoblast (it has been verified in several human organs that connective tissue hardly consumes glucose), one gets $k_g \approx 0.0025 \text{ s}^{-1}$.

Equations 3, 4, 5 involve quite a few parameters whose values can be roughly estimated at best. GLUT1 characteristics in erythrocytes (Lowe and Walmsley 1986; Walmsley et al. 1988; Baldwin 1993) have been measured, but no data regarding MVM or BM are available. Those membranes are much different both by their thickness (Truman et al. 1981; Honda et al. 1992; Jackson et al. 1992) and by their structure (Johnson and Smith 1985; Vanderpuye and Smith 1987; Jansson et al. 1993). GLUT1 expression and activity have been shown to depend on the host cell environment (Cloheroy et al. 1996, Lundqvist and Lundahl 1997, Levine et al. 2005); therefore, we are reluctant to incorporate measured parameter values on “as is” basis in this simulation. Here, we extend on the choice of those parameter values:

* The translocation rate constants at the two membranes are k_{oMVM} and k_{oBM} . These should be at least one order of magnitude higher than P_{0g} and P_{1g} the permeability constants of the membranes with respect to the free glucose reflecting the dominance of the mediated transport.

* The asymmetry of the translocation rates represented by the deviation of prop_{MVM} and prop_{BM} from 1. In vitro measurements indicated on asymmetric inward and outward movements of the glucose-GLUT1 complex

via the erythrocytes membrane (Baldwin 1993; Lundqvist and Lundahl 1997). We suspected that $prop_{MVM}$ and $prop_{BM}$ are close to 1 because of the following reasons: A. When heating from room to body temperature, the asymmetry between the rate constants considerably declines (Baldwin 1993; Lundqvist and Lundahl 1997). B. Smaller than 1 proportion constants imply a diminished effect of the feedback from the fetus as to how much glucose is needed—a non-advisable situation. Moreover, the dependence of the transplacental glucose flux on the maternal-fetal glucose gradient (Desoye et al. 2011) and not on the maternal glucose concentration must be a result of a significant bidirectional transport. Actually, the two membranes might be viewed as a double barrier between mother and fetus where MVM, having about 18-fold GLUT1 compared to BM, is the main “driving force” of glucose supply; thus, $prop_{MVM}$, being the more affecting factor, probably equals 1, while $prop_{BM}$ might be a bit smaller. Nevertheless, we applied other values of $prop_{MVM}$ and $prop_{BM}$ as well.

In addition, computation of the glucose-transporter complex concentrations makes use of

* Dissociation equivalence constants at the two faces of the two membranes, K_{dMVM}^{out} , K_{dMVM}^{in} , K_{dBm}^{out} , and K_{dBm}^{in} . At erythrocytes’ membrane, the exofacial and endofacial conformations have approximately the same affinity to glucose in room temperature (Baldwin 1993, Lundqvist and Lundahl 1997) (about 15 mM), while for body temperature, the affinities of the two conformations differ by a factor of 2.3. We ran the model for a range of parameter values (between 10 and 25 mM at each face of the two membranes).

* The proportion between the exofacial (exo) and endofacial (endo) concentrations. The erythrocytes data reveal that while most of the GLUT1 in low temperatures faces the outward side, body temperature induces almost equal percentages of endofacial and exofacial conformations (Baldwin 1993, Lundqvist and Lundahl 1997). We applied both symmetric (exo = endo = 0.5) and asymmetric distributions of the transporter.

* The unknown concentrations of the transporter at the two membranes. GLUT1 concentration at the MVM, C_{GLUT}^{MVM} equals about 3.2 its value at the BM, C_{GLUT}^{BM} (Barta and Drugan 2010). As it was demonstrated in Barta and Drugan (2010), the fluxes at the membranes are, to a leading order, proportional to the product of GLUT1 concentration by the translocation rate; therefore, a given glucose flux via the MVM actually determines the product of the translocation rate by the GLUT1 concentration there. Here, we use a somewhat arbitrary k_{oMVM} , see Table 3, and then determine C_{GLUT}^{MVM} .

Table 3 Literature based and computed parameter values for the present simulation

Parameter	Value	Reference
Diffusion coefficient for glucose (D)	$3.2 \times 10^{-6} \text{ cm}^2 \text{s}^{-1}$	Barta and Drugan 2010
Rate of metabolic consumption (k_g)	0.0025 s^{-1}	Villee 1953; Ogburn et al. 1988
Maternal blood glucose concentration (C_g^m)	4.75 mM	Barta and Drugan 2010
Fetal vein blood glucose concentration (C_g^f)	4.0 mM	Barta and Drugan 2010
Equilibrium dissociation constant for glucose and GLUT1 at both exofacial and endofacial sites and at both membranes (K_{dMVM}^{in} , K_{dMVM}^{out} , K_{dBm}^{in} , K_{dBm}^{out})	10–25 mM	Lundqvist and Lundahl 1997, Baldwin 1993
Permeability coefficient of MVM to glucose (P_{0g})	$0.3 \times 10^{-6} \text{ cm s}^{-1}$	Barta and Drugan 2010
Permeability coefficient of BM to glucose (P_{1g})	$1.2 \times 10^{-6} \text{ cm s}^{-1}$	Barta and Drugan 2010
Translocation constant for GLUT1-glucose complex at MVM (k_{oMVM})	$4 \times 10^{-5} \text{ cm s}^{-1}$	
Translocation constant for GLUT1-glucose complex at BM (k_{oBM})	$0.5\text{--}30 k_{oMVM}$	
Proportions of endofacial and exofacial GLUT1 sites at both membranes (endo, exo)	0.3–0.7	Lundqvist and Lundahl 1997; Baldwin 1993
Factor that represents asymmetry in translocation rates within the MVM ($prop_{MVM}$)	0.9–1	
Factor that represents asymmetry in translocation rates within the BM ($prop_{BM}$)	0.8–1	

In the future, once C_{GLUT}^{MVM} or k_{oMVM} is measured, its counterpart might be adjusted so as to keep the product close to the value applied here.

Results

We computed the glucose concentration map for the wide range of parameter values listed in Table 3. A set of parameter values is declared as a feasible one if it induces:

1. A physiological glucose uptake. Hauguel et al. (1986) measured in vitro glucose uptake rates by perfusing placental specimens with varied maternal glucose levels, while the fetal glucose level was kept at

Table 4 Ranges of feasible parameter values and the resultant glucose average concentration, \bar{g} . exo = endo unless specified otherwise

$C_{\text{GLUT}}^{\text{MVM}}$ (mM)	$prop_{\text{MVM}}, prop_{\text{BM}}$	$k_{\text{oBM}}/k_{\text{oMVM}}$	$K_{\text{dMVM}}^{\text{in}}$ (mM)	$K_{\text{dMVM}}^{\text{out}}$ (mM)	$K_{\text{dBM}}^{\text{in}}$ (mM)	$K_{\text{dBM}}^{\text{out}}$ (mM)	\bar{g} (mM)
Scenario A							
15–7	1,1	1–3	15	15	15	15	4.63–4.51
Scenario B							
0.38–0.43	1,0.9–1	5–7	23	10	23	10	4.49–4.69
Scenario C							
6–4	1,0.8–1	0.5–0.8	15	15	23	10	4.48–4.38
4.7 ^a	1,1	1	15	15	15	15	4.42
Scenario D							
0.4–0.42	1,0.8–1	15–28	23	10	15	15	4.57–4.71
0.65 ^b	1,1	18	15	15	15	15	4.70

^a at the BM-exo = 0.6, endo = 0.4

^b at the MVM-exo = 0.6, endo = 0.4

constant low level. We adjusted their measured fluxes to the in vivo situation (using physiological C_g^m, C_g^f values) by interpolation and deduced that the glucose uptake is about 0.1 $\mu\text{mol} (\text{min} \times \text{g})^{-1}$ or glucose flux at the MVM of each terminal villus in a 500 g placenta equals $1 \times 10^{-9} \mu\text{mol} \times \text{s}^{-1}$.

2. A consumption of 60–70 % of the glucose uptake (Simmons et al. 1979; Haugel et al. 1986; Jansson et al. 1993) by the placenta (the rest is delivered to the fetus via the BM).
3. An average glucose concentration within the syncytiotrophoblast, \bar{g} that satisfies $0.5(C_g^m + C_g^f) < \bar{g} < C_g^m$ (Johnson and Smith 1980; Barta and Drugan 2010).

Four optional scenarios are distinguished:

- A. Both MVM and BM are symmetric.
- B. Both MVM and BM are highly non-symmetric.
- C. MVM is symmetric, while BM is highly non-symmetric.
- D. BM is symmetric, while MVM is highly non-symmetric.

Asymmetry of a membrane might be a result of one or more of the following conditions: 1) Marked differences between the affinities of the glucose to the GLUT1 at the two faces of the membrane. 2) Uneven distribution of the GLUT1 binding sites or exo \neq endo. 3) Different translocation rates along the in and out directions.

Ranges of feasible sets of values for each of the above scenarios are given in Table 4. All those sets induce concentration maps that satisfy the three constraints specified above. In addition, they all involve low variation of glucose concentration within the syncytiotrophoblast and simple diffusion that plays a minor (at the BM) to negligible (at the MVM) role.

However, those four scenarios involve different GLUT1 concentrations; The assumed, given flux is a function of the gap between the concentrations of the glucose-transporter complex at both faces of membrane, but this gap might be a result of a subtraction of two high, almost identical numbers (e.g., where a membrane is symmetric, and transporter

concentration is high) or two low, much different numbers (e.g., where conditions at both sides of a membrane markedly differ). Since the MVM contains about 18 times GLUT1 compared to the BM, the required transporter concentrations are determined mainly by MVM symmetry characteristics, see Table 4.

On its face, unless more data come from the laboratory and substantiate the value of one or more parameters, one cannot choose between the qualitatively different scenarios described above. However, we suspected that those four optional scenarios might have distinct sensitivities with respect to the conditions that prevail in vivo. Specifically, we checked the effects of raised maternal glucose concentration and of changes in the transporter concentrations (known to occur in the last trimester of pregnancy) on the glucose concentration maps.

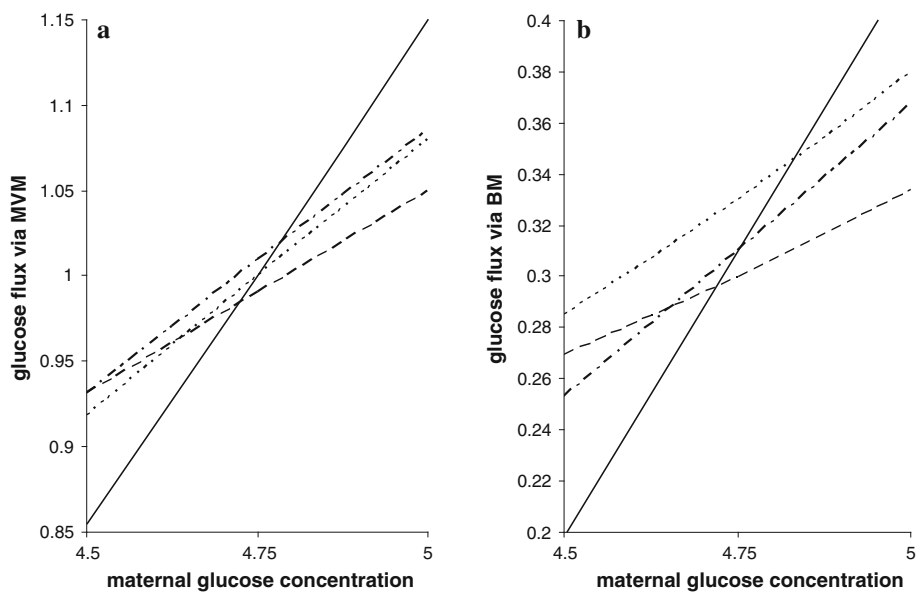
Sensitivity With Respect to Maternal-Fetal Concentration Difference

Doubling the glucose concentration gradient from 0.5 to 1.0 mM (raising C_g^m from 4.5 to 5 mM) induces different effects in the four scenarios, see Fig. 2. Substitution of different sets of parameters within the same category of scenarios results in slightly different sensitivities; however, as long as we confine ourselves to the ranges of parameter values given in Table 4, the qualitatively marked differences between the four scenarios are kept. By comparison of the slopes of the lines in Fig. 2, it is evident that just in scenario A, the concentration gradient is a most crucial factor that highly affects the glucose supply to the fetus, in accord with Desoye et al. (2011).

Sensitivity with respect to transporter densities

$C_{\text{GLUT}}^{\text{BM}}$ significantly increases during the last trimester of pregnancy when the energy requirements are raised, but

Fig. 2 Effect of maternal blood glucose concentration (given in mM) on fluxes (given in $\mu\text{mol} \times \text{s}^{-1}$) via **a** MVM and **b** BM. Scenarios A, B, C, and D are depicted by *solid*, *dashed*, *dotted*, and *dashed-dotted* lines, respectively



$C_{\text{GLUT}}^{\text{MVM}}$ remains almost intact (Jansson et al. 1993; Schneider et al. 2003). This is probably an indication to glucose delivery that is highly sensitive to $C_{\text{GLUT}}^{\text{BM}}$ but is barely sensitive to $C_{\text{GLUT}}^{\text{MVM}}$. Fig. 3 demonstrates the effect of changing transporter concentrations in either (or both) membranes on the glucose delivery. Increasing $C_{\text{GLUT}}^{\text{MVM}}$ has a minor impact only in scenarios A and C. Moreover, only in these scenarios, \bar{g} does not dramatically change when $C_{\text{GLUT}}^{\text{BM}}$ is altered. Although placental glucose concentration was not measured, it seems unlikely that it considerably changes along the pregnancy period. Thus, it is difficult to reconcile scenarios B and D (a non-symmetric MVM membrane) with *in vivo* variations of transporter concentrations along the pregnancy period.

Discussion

We formulated a detailed model of the glucose transport across the terminal villi. Such analytic modeling of the terminal villus might be incorporated in simulations of transport of various other nutrients. Each nutrient, e.g., amino acids, fatty acids, lactate, vitamins, growth regulating hormones, has its own typical mechanism of transport within the two involved membranes (MVM and BM) and its typical metabolic utilization or production rate. Yet, they basically share the same route that has to be crossed (Sibley and Boyd 1979; Gude et al. 2004; Desoye et al. 2011; Benirschke et al. 2012).

The present simulation reveals the role played by each bordering membrane, disguised in one compartmental approach studies (Desoye et al. 2011) where just the total transporters activity is considered. Our computations show

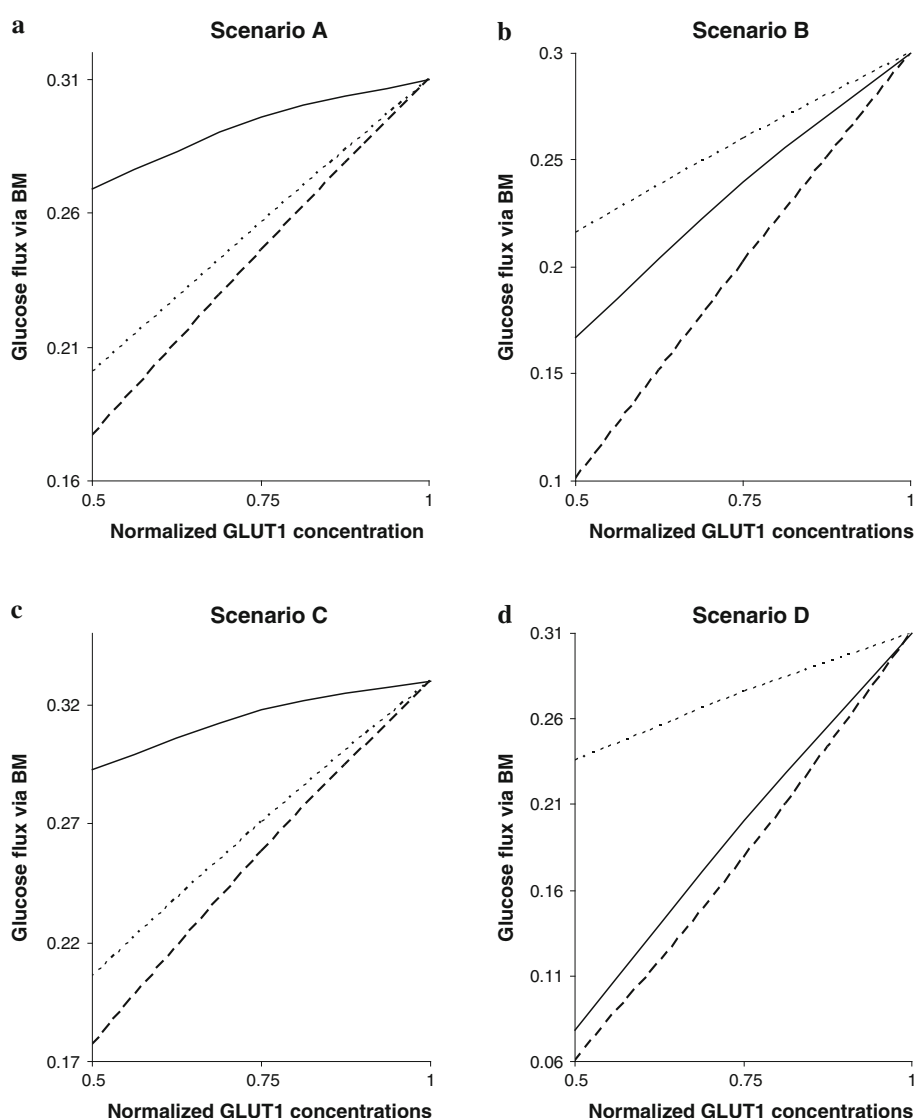
that the MVM is the driving force of the glucose transport, while the BM is the “bottle neck”; thus, the glucose flux that reaches the fetus has much higher sensitivity with respect to the BM characteristics, but on “macro level,” it is determined by the MVM characteristics.

Four different scenarios, representing four optional symmetric conditions at the involved membranes, are determined so as to agree with measurements of glucose fluxes and consumption. Due to the scarcity of measured data, one cannot hope to determine the specific affinities, rate constants, or concentrations of the GLUT1 at the two membranes. However, our model shows that the sensitivity of the transport regime depends mainly on the symmetry properties of the membrane, and it enables choosing the most probable option by comparing theoretical and physiological sensitivities of the glucose fluxes with respect to maternal glucose level and to transporters’ concentrations at the two membranes. It turns out that wherever the MVM is asymmetric, there is no way to reconcile our predictions with observations. In case that both membranes are symmetric, their glucose transport characteristics are quite similar, in accord with Johnson and Smith (1985). Non-symmetric affinity at the BM cannot be overruled but is less likely (as it involves lower sensitivity with respect to the glucose concentration gap). In any case, the transporter is abundant at the two membranes.

The main limitations of this simulation are

* Simplified geometry. Applying the equations for an isolated, spheroidal villus inevitably involves inaccuracies. The effect of neighboring villi and of the flow regime in the intervillous space (Chernyavsky et al. 2010) might be accounted for by substituting (once they are available) varying values of C_g^{m} on the MVM (e.g., glucose concentration in the maternal blood that touches the apex differs

Fig. 3 Effect of GLUT1 concentrations on glucose supply to the fetus in scenarios **a** A, **b** B, **c** C, **d** D. *Dashed, solid, and dotted lines* represent GLUT1 concentrations that change at both membranes, at MVM and at BM, respectively. Concentrations are normalized with respect to the values defined in Table 4. Fluxes are given in $\mu\text{mol} \times \text{s}^{-1}$



from that at the neck of the villus) with no modification of the mathematical simulator.

* Assuming a steady rate of glucose consumption along pregnancy. There is no documentation of a possible change of k_g toward term; however, such a change could affect our sensitivity analysis and our choice of the most probable scenario.

* Skewed parameter values entailed by this simulator due to scarcity of data.

* Simplified GLUT1 activity simulation. Most authors believe that the transport process fits the single site exposure model (Krupka and Deves 1981; Baldwin 1993; Gould and Seatter 1997) and that mechanisms neglected here are of secondary importance. Nevertheless the following assumptions are notable:

- I. Considering just one site for the association of glucose and GLUT1, neglecting the difference between the dimeric and tetrameric GLUT1.

- II. Neglecting acceleration due to glucose presence at the opposite face and inhibition due to the presence of other competitors that bind to GLUT1.

We call the experimentalists to make measurements in MVM and BM as experimental determination of any of the parameter values involved will help to shed light on the transport process by reducing the number of degrees of freedom to choose the right parameter values.

Quite a few measurements indicated on asymmetric affinity of GLUT1 at the only studied membrane: the membrane of erythrocytes. The discrepancy between those reports and our findings might be due to

1. The physiological situation in the placenta where there is a double barrier (two membranes) between glucose supplier (mother) and consumer (fetus) is markedly different from that in the erythrocyte where there is

just one membrane to cross. It might cause those membranes to evolutionary adopt different strategies of facilitation. Moreover, Lundqvist and Lundahl (1997) showed that the affinity of glucose for GLUT1 depends on the lipid bilayer composition; thus, utilizing data obtained for one membrane in a structurally different one might be illegitimate.

- Cloherty et al. (1996) claimed that GLUT1 sugar-mediated transport is an intrinsically symmetric process but that intracellular sugar complexion in human red cells prevents accurate determination of transport rates. Thus, *in vitro* measurements in erythrocytes might not reflect the *in vivo* rates.
- The above mentioned simplifications of this simulation.

We plan to further confront our predictions with physiological situations by implementing this method to different diabetic conditions. We would expect the same scenario (A, B, C, or D) to prevail under different diabetic conditions (albeit with different parameter values); thus, such simulations might corroborate (or not) our conclusions.

References

Aherne W, Dunnill MS (1966) Morphometry of the human placenta. *Br Med Bull* 22(1):5–8

Baldwin S (1993) A. Mammalian passive glucose transporters: members of an ubiquitous family of active and passive transport proteins. *Biochim Biophys Acta* 1154:17–49

Barta E, Drugan A (2010) Glucose transport from mother to fetus—a theoretical study. *J Theor Biol* 263(3):295–302

Baumann MU, Deborde S, Illsley NP (2002) Placental glucose transfer and fetal growth. *Endocrine* 19(1):13–22

Benirschke K, Burton GJ, Baergen RN (2012) Pathology of the Human Placenta, 6th edn. Springer, Berlin

Chernyavsky IL, Jensen OE, Leach L (2010) A mathematical model of intervillous blood flow in the human placentone. *Placenta* 31:44–52

Cloherty EK, Heard KS, Carruthers A (1996) Human erythrocyte sugar transport is incompatible with available carrier models. *Biochemistry* 35:10411–10421

Day PE, Cleal JK, Lofthouse EM, Hanson MA, Lewis RM (2013) What factors determine placental glucose transfer kinetics? *Placenta* 34(10):953–958

Demir R (1979) Scanning electron-microscopic observations on the surfaces of chorionic villi of young and mature placentas. *Acta Anat* 105:226–232

Desoye G, Gauster M, Wadsack C (2011) Placental transport in pregnancy pathologies. *Am J Clin Nutr* 94(suppl):1896S–1902S

Gould GW, Seatter MJ (1997) Introduction to the facilitative glucose transporter family. In: Gould GW (ed) Facilitative Glucose Transporters. Springer-Verlag, Heidelberg, pp 1–37

Gude NM, Roberts CT, Kalionis B, King RG (2004) Growth and function of the normal human placenta. *Thromb Res* 114:397–407

Haugel S, Desmaizieres V, Challier JC (1986) Glucose uptake, utilization, and transfer by the human placenta as functions of maternal glucose concentration. *Pediatr Res* 20:269–273

Hay WW, Molina RA, DiGiacomo JE, Meschia G (1990) Model of placental glucose consumption and glucose transfer. *Am J Physiol.* 258(Regulatory Integrative Comp. Physiol. 27): R569–577

Higgins M, Felle P, Mooney EE, Bannigan J, McAuliffe FM (2011) Stereology of the placenta in type 1 and type 2 diabetes. *Placenta* 32:564–569

Honda M, Toyoda C, Nakabayashi M, Omori Y (1992) Quantitative investigations of placental terminal villi in maternal diabetes mellitus by scanning and transmission electron microscopy. *Tohoku J Exp Med* 167:247–257

Ibrahim MEA, Al-Zuhair AGH, Mughal S, Hathout H (1982) Surface ultrastructure of the human placental villi and sites of contact with maternal red blood cells. *Arch Gynecol* 233:67–72

Jackson MR, Mayhew TM, Boyd PA (1992) Quantitative description of the elaboration of villi from 10 weeks of gestation to term. *Placenta* 13:357–370

Jansson T, Wennergren M, Illsley NP (1993) Glucose transporter protein expression in human placenta throughout gestation and in intrauterine growth retardation. *J Clin Endocrinol Metab* 77:1554–1562

Jansson T, Wennergren M, Powell TL (1999) Placental glucose transport and GLUT1 expression in insulin-dependent diabetes. *Am J Obstet Gynecol* 180:163–168

Jauniaux E, Burton GJ (2006) Villous histomorphometry and placental bed biopsy investigation in type 1 diabetic pregnancies. *Placenta* 27:468–474

Jirkovska M, Kubinova L, Krekule I, Hach P (1998) Spatial arrangement of fetal placental capillaries in terminal villi: a study using confocal microscopy. *Anat Embryol* 197:263–272

Jirkovska M, Janacek J, Kalab J, Kubinova L (2008) Three-dimensional arrangement of the capillary bed and its relationship to microrheology in the terminal villi of normal term placenta. *Placenta* 29:892–897

Jirkovska M, Kucera T, Kalab J, Jadrnicek M, Niedobova V, Janacek J, Kubinova L, Moravcova M, Zizka Z, Krejci V (2012) The branching pattern of villous capillaries and structural changes of placental terminal villi in type 1 diabetes mellitus. *Placenta* 33:343–351

Johnson LW, Smith CH (1980) Monosaccharide transport across microvillous membrane of human placenta. *Am J. Physiol.* 238 (Cell Physiol. 7):C160–168

Johnson LW, Smith CH (1985) Glucose transport across the basal membrane of human placental syncytiotrophoblast. *Biochim Biophys Acta* 815:44–50

Karimu AL, Burton GJ (1995) The distribution of microvilli over the villous surface of the normal human term placenta is homogeneous. *Reprod Fertil Dev* 7:1269–1273

Krupka RM, Deves R (1981) An experimental test for cyclic versus linear transport models. The mechanism of glucose and choline transport in erythrocytes. *J Biol Chem* 256(11):5410–5412

Laga EM, Driscoll SG, Munro HN (1973) Quantitative studies of human placenta I Morphometry. *Biol Neonate* 23:231–259

Levine KB, Robichaud TK, Hamill S, Sultzman LA, Carruthers A (2005) Properties of the human erythrocyte glucose transport protein are determined by cellular context. *Biochemistry* 44:5606–5616

Lowe AG, Walmsley AR (1986) The kinetics of glucose transport in human red blood cells. *Biochim Biophys Acta* 857:146–154

Lundqvist A, Lundahl P (1997) Glucose affinity for the glucose transporter Glut1 in native or reconstituted lipid bilayers temperature-dependence study by biomembrane affinity chromatography. *J Chromatogr A* 776:87–91

Mayhew TM (2003) Stereological studies on fetal vascular development in human placental villi. *Image anal Stereol* 22:49–56

Mayhew TM, Sorensen FB, Klebe JG, Jackson MR (1994) Growth and maturation of villi in placenta from well-controlled diabetic women. *Placenta* 15:57–65

Ogburn PL Jr, Rejeshwari M, Turner SI, Hoegsberg B, Haning RV (1988) Lipid and glucose metabolism in human placental culture. *Am J Obstet Gynecol* 159(3):629–635

Schneider H, Reiber W, Sager R, Malek A (2003) Asymmetrical transport of glucose across the in vivo perfused human placenta. *Placenta* 24:27–33

Sen DK, Kaufmann P, Schweikhart G (1979) Classification of human placental villi II Morphometry. *Cell Tissue Res* 200:425–434

Sibley CP, Boyd DH (1979) Mechanisms of transfer across the human placenta. In: Polin Fox (ed) *Fetal and Neonatal Physiology*, vol 1. W. B Saunders Company, Philadelphia, pp 62–74

Simmons MA, Battaglia FC, Meschia G (1979) Placental transfer of glucose. *J Dev Physiol* 1:227–243

Teasdale F, Jean-Jacques G (1985) Morphometric evaluation of the microvillous surface enlargement factor in the human placenta from mid-gestation to term. *Placenta* 6:375–381

Truman P, Wakefield J, Ford HC (1981) Microvilli of the human term placenta. *Biochem J* 196:121–132

Vanderpuye OA, Smith CH (1987) Proteins of the apical and basal plasma membranes of the human placental syncytiotrophoblast: immunochemical and electrophoretic studies. *Placenta* 8:591–600

Villee CA (1953) The metabolism of human placenta in vitro. *J Biol Chem* 205:113

Walmsley AR, Barrett MP, Bringaud F, Gould GW (1988) Sugar transporters from bacteria, parasites and mammals: structure-activity relationships. *Trends Biochem Sci* 23(12):476–481